J Solid State Electrochem (2012) 16:2867–2876
DOI 10.1007/s10008-012-1717-4

ORIGINAL PAPER

Electrochemical studies of nafion–trimethylsilyl and nafion–trimethylsilyl/Ru complex-modified electrodes

Rocío Aguilar-Sánchez · Rodrigo J. Díaz-Caballeros · J. Antonio Méndez-Bermúdez · J. Luis Gárate-Morales · Guadalupe Domínguez-Meneses

Received: 5 January 2012 / Revised: 1 March 2012 / Accepted: 5 March 2012 / Published online: 20 March 2012

Abstract In this work, we report the electrochemical properties of the nafion–trimethylsilyl (Naf–TMS) polymer. First, we introduce a procedure to dissolve Naf–TMS polymer and the incorporation of ruthenium catalyst complexes into it. The inclusion of the catalysts involved two strategies. The first one concerned the direct formation of a Naf–TMS/Ru complex solution. The second one consists of depositing Naf–TMS solution on a glassy carbon electrode, followed by the incorporation of Ru complexes under potentiodynamic conditions. Electrochemical studies showed the good ion permeation capability of Naf–TMS membranes and its use as a good alternative approach to Nafion ion-conducting membranes. The analytical capabilities of Naf–TMS- and Naf–TMS/Ru-modified glassy carbon electrodes have been tested for the detection of dopamine in standard solutions. Detection limits in the order of nanomolar have been achieved with working ranges extending over three decades in concentration at pH 7.2. Further enhancement in the dopamine oxidation current was achieved by the incorporation of Ru complexes into the Naf–TMS polymer. This study offers a new insight into the investigation of Naf–TMS resin as an ion-conducting polymer.

Keywords Nafion–TMS · $Ru[(CN)_6]^{4-}$ · $Ru[(phen)_3]^{2+}$ · $Ru[(bpy)_3]^{2+}$ · Dopamine · Glassy carbon electrodes

R. Aguilar-Sánchez (✉) · R. J. Díaz-Caballeros · J. L. Gárate-Morales · G. Domínguez-Meneses
Depto. Química Analítica, Facultad de Ciencias Químicas, Benemérita Universidad Autónoma de Puebla, 72570 Puebla, Mexico
e-mail: raguilar@ifuap.buap.mx

J. A. Méndez-Bermúdez
Instituto de Física, Benemérita Universidad Autónoma de Puebla, 72570 Puebla, Mexico

Introduction

The modification of electrode surfaces by polymers provides a unique opportunity to immobilize catalyst and thereby extends the electrochemical methodology to systems where promotion of charge transfer is required. Electroactive catalysts can be bound quite readily to an electrode surface by using a polymer layer. So far, perfluorinated ionomer membranes have attracted great interest as a result of their intrinsic properties such as ion exchange selectivity, thermal stability and chemical–biological inertness. Also, they are promising as matrixes for functional molecules and as electrolytes. Among the family of perfluorinated ionomers, Nafion® has been extensively studied primarily because it has proved to be particularly useful in confining large quantities of catalyst in the form of transition metal complexes [1–4]. Nafion® has a number of applications as a proton exchange membrane in fuel cells [5], in photovoltaic cells [6] as an electrode modifier [1, 7, 8] and in ion-selective electrodes [9] and voltammetric sensors [10]. Frequently, the rate of the process involved in these applications entails a rapid charge and mass transport through the polymer. However, an unfortunate low diffusion process of some chemical species in the Nafion® films has the undesirable effect of increasing the response time of the electrode [11]. In this regard, the development and exploration of new polymeric solid materials is necessary to establish fast charge and molecular transport for future applications.

From previous studies [12], three regions have been distinguished in the matrix of Nafion®, which include semicrystalline-type portions combined with non-crystalline areas in which the anionic sulfonate groups are aggregated. It has been shown that Nafion® in the hydrogen ion form is an effective solid "superacid" catalyst for a variety of organic reactions [13]. The highly acidic sulfonic group of Nafion® is very reactive, which makes it

a good reaction site where inorganic phases can be grown [14]. Based on these properties, Murata and Noyori [15] first reported the preparation of Nafion–trimethylsilyl for which they suggested the name nafion–TMS (Naf–TMS), which is a polymer-supported silylating agent (Scheme 1).

On the other hand, the incorporation of redox centre molecules in polymer membranes as Nafion® represents a very promising approach to enhance charge transport and produce functional materials with desirable redox, optical and electrocatalytic properties. Immobilization of materials such as Ru(II) and Ru(III) complexes, at modified electrode surfaces, has found their possible application as highly sensitive and selective electroluminescence sensors [16, 17], glucose biosensors [18], and biochemical sensors [19] and these have also been introduced as a light-harvesting material in hybrid photovoltaic cells [6]. Moreover, polymeric solid resins show potential as electrolytes. In electrochemical sensing, the partitioning of an analyte into the polymer film is a process that is fundamental. In these cases, a rapid charge and molecular transport is compulsory for an efficient work.

Nafion® is the most common and currently studied perfluorosulfonated material. Nevertheless, it has problems associated to its low operating temperature limit, it is expensive and it has a relatively high methanol permeability which limits its application in fuel cells. These are factors that still limit its wide-scale use. Several alternatives have been developed but have not been further investigated. In the present study, we report a method to dissolve nafion–trimethylsilyl resin and its modification with Ru complexes from two methods. The modified electrodes showed good ion permeation to cations and fast response. Furthermore, we studied the analytical response of Naf–TMS and Naf–TMS/Ru complex-modified electrodes to detect dopamine (DA) in standard solutions, which is an important cathecolamine-type neurotransmitter. To the best of our knowledge, no report which addresses the capability of polymer Naf–TMS to confine catalyst and its role to detect and promote biological substances as DA is available. The analytical response of Naf–TMS-modified electrodes might be particularly relevant to electrochemical biosensors, fuel and photovoltaic cells.

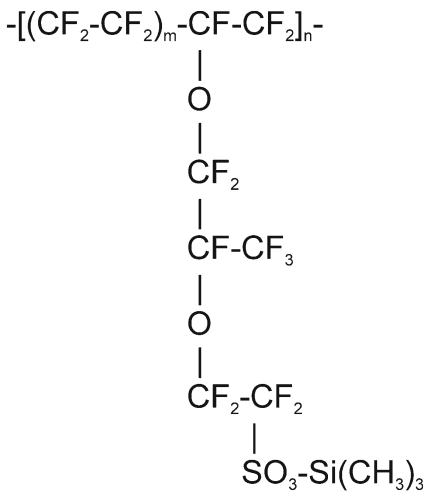

Scheme 1 Chemical structure of the Naf–TMS polymer [15]

Experimental

Chemicals

Dopamine (Sigma), CH_3CH_2OH (Baker), H_2SO_4 (Merck), $HNa_2PO_4{\cdot}12H_2O$ (Merck), $H_2NaPO_4{\cdot}H_2O$ (Merck) and KCl (Merck) were all of reagent grade and used as received without any further purification. Ruthenium complexes—$K_4[Ru(CN)_6]$ ($[Ru(CN)_6]^{4-}$, potassium hexacyanoruthenate(II) hydrate), $C_{36}H_{24}Cl_2N_6Ru{\cdot}xH_2O$ ($[Ru(phen)_3]^{2+}$, dichlorotris (1,10-phenanthroline) ruthenium(II) hydrate, 98 %), $C_{30}H_{24}Cl_2N_6Ru{\cdot}6H_2O$ ($[Ru(bpy)_3]^{2+}$ Tris (2,2′-bipyridyl) ruthenium(II) chloride hexahydrate)—and Naf–TMS were from Sigma-Aldrich. All solutions were prepared with Milli-Q water (18.2 MΩ) before each experiment. The working solutions were obtained by appropriate dilution in 0.1 M H_2SO_4 or phosphate buffer solution (PBS) of corresponding pH. Nafion–TMS was purchased from Sigma-Aldrich (0.5 meq) in the form of polymer pellets.

Naf–TMS dissolution process

We have found that Naf–TMS is very resistant to chemical attack, even by strong oxidants at elevated temperature, and organic solvents. It has been well documented [20] that perfluorinated polymers interact much more strongly with binary solvent systems. Then, dissolution of these polymers should be more compliant by using two solvents. Naf–TMS was dissolved in a 50:50 ethanol–water mixture. The procedure for preparation of 1 wt/vol % solution was as follows: 1 g of small pellets of the as-received polymer was transferred to a beaker containing the solvent and it was placed in an ultrasonic bath for approximately 1 h, until the yellow shade of the as-received polymer vanished. After this treatment, the polymer pellets were moved to a containing solvent high-pressure reactor, purged with Ar, and heated at 250 °C for 2 h. The obtained solution was slightly viscous and transparent. The GC electrodes were modified with this solution.

Supporting of $Ru[(CN)_6]^{4-}$ and $Ru[(phen)_3]^{2+}$ in Naf–TMS polymer

Two methods were used to incorporate Ru complexes into the polymer: method 1—the incorporation of the ruthenium complex was carried out under potentiodynamic conditions after the Naf–TMS film formation on the electrode surface

and method 2—incorporation before film preparation (one-step method). The former method involved deposition of an aliquot of the corresponding Naf–TMS polymeric solution onto a glassy carbon surface, allowing the solvent to evaporate at room temperature. Then, the electrode was immersed in an electrochemical cell with a Ru complex-containing solution and the potential was scanned at 100 mV s^{-1}. In the one-step method, a mixture either of $K_4[Ru(CN)_6]$ ($[Ru(CN)_6]^{4-}$) or $C_{36}H_{24}Cl_2N_6Ru{\cdot}xH_2O$ ($[Ru(phen)_3]^{2+}$) and previously hydrated Naf–TMS pellets (Aldrich) was heated in a sealed oxygen-free container for 2 h at 250 °C, employing a 50:50 mixture of ethanol–water as solvent. The obtained solution was used to modify the GC electrode. The presence of ruthenium in the Naf–TMS matrix was confirmed by infrared (IR) spectroscopy of films prepared from the Naf–TMS/Ru complex polymeric solution.

Electrode preparation

A glassy carbon electrode was used as substrate to deposit Naf–TMS and Naf–TMS/Ru complex. First, the electrode was polished using diamond paste of 3 and 0.25 μm diameter successively, followed by rinsing with acetone and later cleaned abundantly with deionized water (Milli-Q water, 18 MΩ) for several times in an ultrasonic bath. The method to prepare a GC-coated electrode involves deposition of an aliquot of the corresponding Naf–TMS or Naf–TMS/Ru complex polymeric solution onto the electrode surface, and then the solvent was allowed to evaporate at room temperature.

Electrochemical measurements

The electrochemical measurements were performed with an Epsilon (Bioanalytical Systems) potentiostat–galvanostat. The BASi-Epsilon EC (ver. 2.13.77) software was used for control and data acquisition. A three-electrode glass cell was employed. The GC, GC/Naf–TMS and GC/Naf–TMS/Ru complex were used as working electrodes, the counter electrode was a Pt wire and a mercury–mercury sulfate ($Hg/HgSO_4$, saturated solution) electrode served as reference. The parameters used for differential pulse voltammetry (DPV) were a scan rate of 20 mV s^{-1} and a pulse modification of 50 mV in amplitude, 50 ms in duration at intervals of 200 ms.

Infrared spectroscopy of Naf–TMS samples

The infrared spectra were recorded on a Digilab Varian spectrophotometer. All IR spectra were measured in KBr (Merck, IR spectroscopic grade), employing the transmission technique. Before the measurements, KBr was mixed with freshly prepared solutions of Naf–TMS or Naf–TMS/Ru complex, and the mixture was dried at 90 °C during 24 h. The films for IR spectroscopy were prepared from this mixture.

Results and discussion

IR spectroscopy of Naf–TMS and Naf–TMS/Ru complex samples

In order to show the preservation of the polymer after the dissolution process and to demonstrate the presence of Ru complexes into the Naf–TMS resin, we carried out a series of IR spectroscopy studies. The infrared spectra of Naf–TMS and Naf–TMS/Ru prepared according to method 2 are shown in Fig. 1. The spectral features observed were well reproducible between different samples prepared by the same method. The spectrum of Naf–TMS is very similar for that reported [21] for a K^+ salt of Nafion (Fig. 1a). In the range between 1,400 and 500 cm^{-1}, six very strong vibration bands are present; the assignment can be made by comparison with previous reports [21, 22]. The band observed at approximately 1,230 cm^{-1} can be attributed to asymmetric C–F stretching, while the band at 1,154 cm^{-1} is attributed to symmetric C–F stretching [22]. These bands are overlapped, suggesting several contributions arising from the C–F bond embedded in different structural environments.

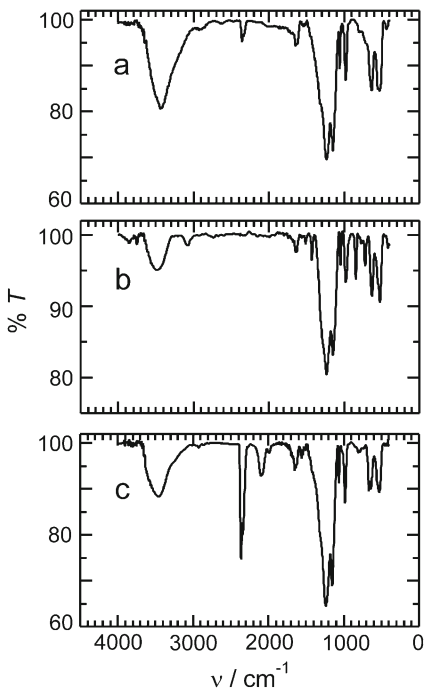

Fig. 1 Infrared spectra of Naf–TMS and Naf–TMS/Ru complex in KBr. **a** Naf–TMS, **b** Naf–TMS/$[Ru(phen)_3]^{2+}$ and **c** Naf–TMS/$[Ru(CN)_6]^{4-}$

In the region from 1,100 to 500 cm^{-1}, a very sharp band appeared at~980 cm^{-1}. According to Laporta et al. [22] and Ostrowska and Narebska [23], this band arises from the C–F stretching of (CF–CF(R)–CF3) groups. Also, a very sharp adsorption band can be observed at ~1,060 cm^{-1}. From previous reports, one can assign this band to the –S–O stretching adsorption [21]. The band at 636 cm^{-1} is due to the stretching of C–S groups according to [24].

In the infrared spectrum of the dried Naf–TMS/Ru $[(phen)_3]^{2+}$ sample, absorption bands in the C–F stretching frequency could also be detected (Fig. 1b). The analysis of the spectrum is greatly aided by comparison with spectra reported before [25]. In the fingerprint region (1,300–1,800 cm^{-1}), the infrared spectrum showed a small absorption which is distinguished at around 1,430 cm^{-1}. Such band corresponds to the stretching bands (C=C and C=N) of phenantroline ligand according to [25]. The additional bands observed at approximately 848 and 721 cm^{-1} are mainly due to the ligand vibrations slightly perturbed by coordination.

The infrared spectrum of $[Ru(CN)_6]^{4-}$-modified Naf–TMS is shown in Fig. 1c. Basically, all the Naf–TMS features are preserved, with an additional absorption band at 2,096 cm^{-1} which can be correlated to the CN group [26] based on compounds containing a $M^{2+}(CN)_6$ fragment [27]. The CN frequency values are typically assigned to the presence of M^{2+} metal ions [28, 29].

Voltammetric response as a function of Ru loading time for Naf–TMS-coated electrodes (method 1)

Figure 2 shows a series of potentiodynamic responses for Naf–TMS-coated GC electrodes as they were immersed in an aqueous solution containing 1×10^{-4} M ruthenium complexes as redox probes: (a) $[Ru(bpy)_3]^{2+}$, (b) $[Ru(phen)_3]^{2+}$ and (c) $[Ru(CN)_6]^{4-}$, respectively. Curves were performed under loading conditions in different electrolytes (0.1 M H_2SO_4 and 0.1 M KCl) at a scan rate of 100 mV/s.

From Fig. 2a, the incorporation of $[Ru(bpy)_3]^{2+}$ was clearly fast as the maximum current was reached in only a few scans (approximately 2 min) and remained virtually constant by repeated cycling. According to a previous work [1], incorporation of the same species in Nafion® films took at least 20 min until a steady-state voltammogram was obtained. The faster increase in voltammetric response can be attributed to the faster diffusion of $[Ru(bpy)_3]^{2+}$ in Naf–TMS than in Nafion® films. As a result of the diffusion tail, forward and backward scans showed anodic peaks slightly larger than the respective cathodic ones. The observed oxidation and reduction peaks are broad and separated by about 120 mV. For Nafion® films, this value was about 100 mV.

The incorporation of $[Ru(bpy)_3]^{2+}$ is markedly faster than that observed for $[Ru(phen)_3]^{2+}$. Cyclic voltammograms for

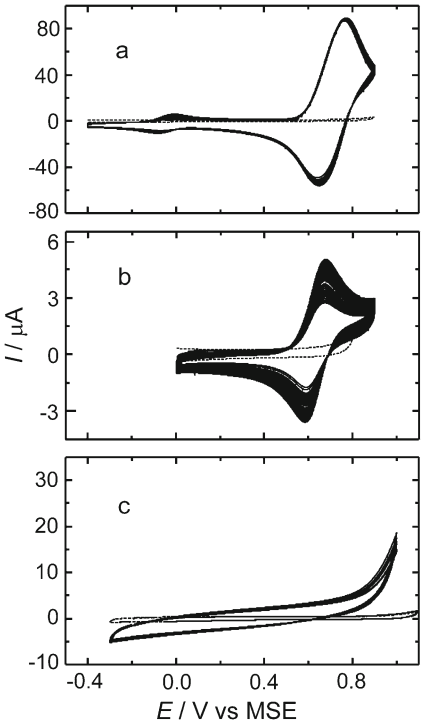

Fig. 2 Cyclic voltammograms recorded continuously for Naf–TMS-modified glassy carbon electrodes immersed in a solution containing different ruthenium complexes. **a** 1×10^{-4} M $[Ru(bpy)_3]^{2+}$ (supporting electrolyte, 0.1 M H_2SO_4), **b** 1×10^{-4} M $[Ru(phen)_3]^{2+}$ (supporting electrolyte, 0.1 M H_2SO_4), **c** 1×10^{-4} M $[Ru(CN)_6]^{4-}$ (supporting electrolyte, 0.1 M KCl). Scan rate, 100 mV s^{-1}

the incorporation of $[Ru(phen)_3]^{2+}$ into Naf–TMS exhibited continuous increasing of anodic and cathodic peaks with immersion time as the electroactive species was loaded into the film (Fig. 2b). A steady-state voltammogram was obtained at about 20 min of cycling when a maximum peak current was reached. The peak currents obtained are much smaller than those obtained with $[Ru(bpy)_3]^{2+}$. The anodic and cathodic peaks are broad and separated by about 104 mV at a scan rate of 100 mV/s (see Table 1), which is far from the expected value for a Nerstian behaviour. A large ΔE value usually indicates slow heterogeneous electron transfer. Also, the diffusional tail suggested that some redox-electrogenerated sites remained in the layer adjacent to the electrode surface due to a relatively slow transport in the polymer film.

The slower incorporation of the $[Ru(phen)_3]^{2+}$ complex into the film, compared to $[Ru(bpy)_3]^{2+}$, correlates well with its size, shape [30, 31] and hydrophobicity [32]. As the ligand of the complex become more hydrophobic, it interacts strongly with Naf–TMS and consequently it diffuses slowly through the film, indicating that electron transfer between bound $[Ru(phen)_3]^{2+}$–Naf–TMS and the electrode surface is slow. From the observed behaviour, we could anticipate a lower diffusion coefficient (D) of the $[Ru(phen)_3]^{2+}$ complex inside the film (see Table 1). Also,

Table 1 Electrochemical characteristics from cyclic voltammetry of Naf–TMS and Naf–TMS/Ru complex-modified glassy carbon electrodes in the presence of two ruthenium redox probes (supporting electrolyte, 0.1 M H_2SO_4)

[a]Scan rate, 100 mV/s

Electrode modifier	Analyte	ΔE^a (mV)	D (cm^2/s)	Γ (mol/cm^2)
Naf–TMS	0.1 mM $[Ru(bpy)_3]^{2+}$	120±5	$(1.7\pm0.2)\times10^{-3}$	$(3.5\pm0.5)\times10^{-9}$
Naf–TMS/$[Ru(phen)_3]^{2+}$	0.1 mM $[Ru(bpy)_3]^{2+}$	150±4	$(4.4\pm0.4)\times10^{-6}$	$(1.4\pm0.1)\times10^{-10}$
Naf–TMS/$[Ru(CN)_6]^{4-}$	0.1 mM $[Ru(bpy)_3]^{2+}$	97±4	$(6.5\pm0.5)\times10^{-4}$	$(1.2\pm0.1)\times10^{-9}$
Naf–TMS	0.1 mM $[Ru(phen)_3]^{2+}$	104±3	$(1.6\pm0.4)\times10^{-5}$	$(4.8\pm0.2)\times10^{-11}$
Naf–TMS/$[Ru(phen)_3]^{2+}$	0.1 mM $[Ru(phen)_3]^{2+}$	79±5	$(4.5\pm0.5)\times10^{-7}$	$(1.1\pm0.2)\times10^{-11}$
Naf–TMS/$[Ru(CN)_6]^{4-}$	0.1 mM $[Ru(phen)_3]^{2+}$	110±10	$(1.4\pm0.5)\times10^{-5}$	$(1.5\pm0.2)\times10^{-11}$

discrepancies in the interaction of $[Ru(bpy)_3]^{2+}$ and $[Ru(phen)_3]^{2+}$complexes with other systems have been reported [33]. Currently, we are carrying out spectro-electrochemical experiments and, at the moment, we have observed a slower inclusion of $[Ru(phen)_3]^{2+}$ into Naf–TMS compared to $[Ru(bpy)_3]^{2+}$.

The electrochemical loading of the $[Ru(CN)_6]^{4-}$ complex into the Naf–TMS film was not detected as a diffusional peak (Fig. 2c). In view of the fact that a similar behaviour was also observed with other anions such as $[Fe(CN)_6]^{3-}$, we can hypothesize that this can be due to a less affinity of Naf–TMS for anions or to the more hydrophilic nature of this Ru complex. The later may favour its incorporation only in the hydrophilic domain of Naf–TMS. Nevertheless, by the one-step method, the incorporation of the complex was confirmed by IR spectroscopy.

For Naf–TMS films in contact with 1×10^{-4} M $[Ru(bpy)_3]^{2+}$ in 0.1 M H_2SO_4, the anodic peak currents were proportional to $v^{1/2}$, indicating that the current was controlled by diffusion in the layers (Fig. 3). From the slope of the plot shown as the inset in Fig. 3 and by the use of Randles–Sevcik equation [34], D was calculated giving a value of 1.7×10^{-3} cm^2 s^{-1}. Such a large value would indicate a highly enhanced ion transport and a fast diffusion of the reactant through the film. The diffusion coefficients of redox species in solid macromolecules have been very similar to those in aqueous solvents. For example, it has been reported that redox molecules diffuse rapidly in solid agarose and κ-carrageenan [35], which implies that molecular diffusion of the redox moieties takes place in solids much like in aqueous solution. This represents a clear advantage compared to Nafion® films [1].

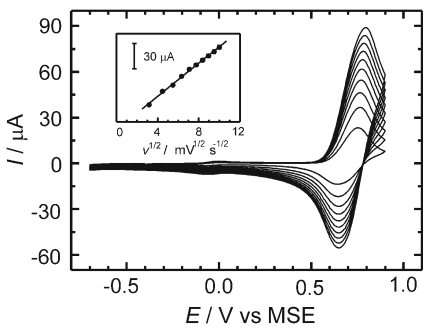

Fig. 3 Cyclic voltammograms recorded at various scan rates at a Naf–TMS-modified glassy carbon electrode in 0.1 M H_2SO_4 in the presence of 1×10^{-4} M $[Ru(bpy)_3]^{2+}$. *Inset*, linear dependence of anodic peak current on square root of scan rate

The surface concentration (Γ) of loaded $[Ru(bpy)_3]^{2+}$ was calculated by integrating the charge under the peak and using the following equation:

$$\Gamma = \frac{Q}{nFA} \quad (1)$$

where Q is the charge on the forward or reverse scan in Coulombs, n is the number of electrons transferred, F is the Faraday constant (96,486 $Cmol^{-1}$) and A is the geometric area of the electrode (0.2827 cm^2). By following this relation, the obtained value for loaded $[Ru(bpy)_3]^{2+}$ was $\Gamma=(3.5\pm0.5)\times10^{-9}$ mol/cm^2 (Table 1).

Ru complexes incorporated into Naf–TMS polymer by method 2 (one-step method): effect of Ru complex in the diffusion coefficient of a redox probe

In an attempt to study the charge propagation through Naf–TMS-coated electrodes, we carried out electrochemical studies with polymer-bound Ru complexes into Naf–TMS films and studied their response in the presence of Ru complexes or other redox probes in solution. The immobilization of the ruthenium complexes into Naf–TMS was carried out by the one-step method and the electrode surfaces were prepared by depositing an aliquot of the Naf–TMS/Ru complex solution and allowing the solvent to evaporate at room temperature. The electrochemical responses of the GC/Naf–TMS/$[Ru(phen)_3]^{2+}$- and GC/Naf–TMS/$[Ru(CN)_6]^{4-}$-modified electrodes in supporting electrolyte are presented as dashed lines in Fig. 4a, b respectively. Clearly, $[Ru(phen)_3]^{2+}$ was incorporated into Naf–TMS as can be seen from the peak observed (dashed line, Fig. 4a) in blank electrolyte (0.1 M H_2SO_4). In the case of $[Ru(CN)_6]^{4-}$ complex, we could not observe any diffusional peak (dashed line, Fig. 4b); however, its presence inside the Naf–TMS film was confirmed by IR spectroscopy (Fig. 1c).

With the addition of 0.1 mM $[Ru(bpy)_3]^{2+}$ to the supporting electrolyte, both GC/Naf–TMS/$[Ru(phen)_3]^{2+}$ and GC/Naf–TMS/$[Ru(CN)_6]^{4-}$ electrodes showed an

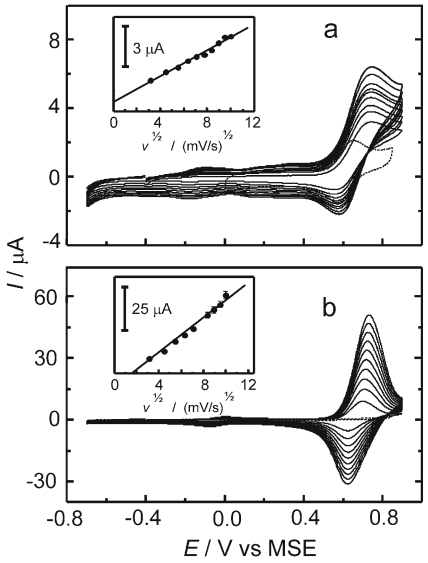

Fig. 4 Series of cyclic voltammograms measured at different scan rates using **a** Naf–TMS/$[Ru(phen)_3]^{2+}$ and **b** Naf–TMS/$[Ru(CN)_6]^{4-}$-modified glassy carbon electrodes in 0.1 M H_2SO_4 in the presence of 1×10^{-4} M $[Ru(bpy)_3]^{2+}$. *Inset*, linear dependence of anodic peak current on square root of scan rate

increase in the peak current (Fig. 4a, b respectively). It is evident that, even in the presence of cationic species and high possibilities of electrostatic repulsion, the GC/Naf–TMS/$[Ru(phen)_3]^{2+}$ electrode still allows the diffusion of another cationic species into the host matrix, although the intensity of the peak is about one order of magnitude less than the electrode modified with Naf–TMS only. The anodic peak current was linearly proportional to the square root of the scan rate (inset Fig. 4a). From this relation, we calculated D (Table 1) and the obtained value was three orders of magnitude smaller than that in Naf–TMS.

In the case of the GC/Naf–TMS/$[Ru(CN)_6]^{4-}$ electrode, there was a significant increase in both the anodic and cathodic currents observed for $[Ru(bpy)_3]^{2+}$ compared to the GC/Naf–TMS/$[Ru(phen)_3]^{2+}$ surface. Also, for this electrode, we observed the smallest ΔE and the fastest electron transfer for $[Ru(bpy)_3]^{2+}$ (97±4 mV; see Table 1). Based on these observations, we speculate that the redox reaction occurring at the Naf–TMS/$[Ru(CN)_6]^{4-}$-modified electrode is probably driven by a balance among hydrophobic attraction, electrostatic binding and ion water solubility. The voltammograms are asymmetric with the cathodic peak being smaller than the anodic peak, clearly indicating differences in diffusion coefficients for $[Ru(bpy)_3]^{2+}$ and the electrogenerated $[Ru(bpy)_3]^{3+}$. In the oxidation of the 2+ to the 3+ complex, the electrostatic interaction between the complex $[Ru(bpy)_3]^{2+}$ and the anionic $[Ru(CN)_6]^{4-}$ seems to be stronger. Nevertheless, on reduction, this interaction becomes weaker, which makes $[Ru(bpy)_3]^{3+}$ diffuse slowly in the polymer film. The scan rate dependence is shown as inset in Fig. 4b. The good linearity of the plot allowed us to determine the value of D to be $6.5\pm0.5\times10^{-4}$ cm^2/s.

In order to further understand the charge transport mechanism within and through the system, currently we are performing spectro-electrochemical measurements. Charge transport can be understood as diffusion of charges in the matrix, charge hopping between redox centres or a combined mechanism where hydrophobic and electrostatic interactions play an important role [36].

Electrochemical oxidation of DA at GC/Naf–TMS and GC/Naf–TMS/Ru complex electrodes in phosphate buffer solution at pH 7.2

The analytical capabilities of Naf–TMS and Naf–TMS/Ru complex-modified electrodes were evaluated by measuring the peak current as a function of a redox probe concentration. In this case, we explore the analytical electrode response using dopamine as a redox probe. Figure 5a shows the first scan of a series of differential pulse voltammograms at a GC/Naf–TMS-modified electrode obtained for DA concentration ranging from 0.9 to 20 μM in phosphate buffer solution at pH 7.2. The

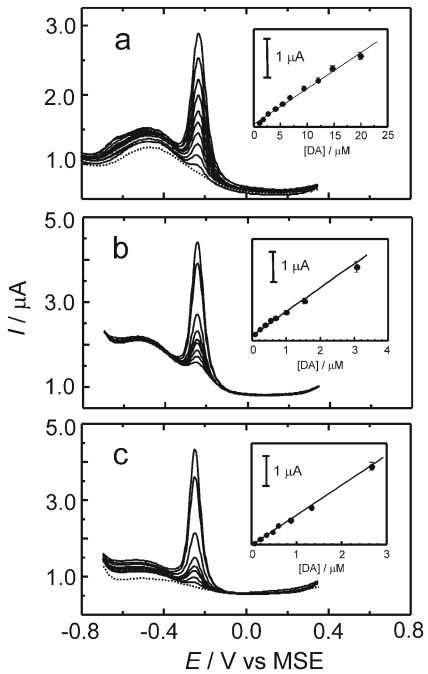

Fig. 5 Differential pulse response obtained for several concentrations of dopamine in phosphate buffer solution pH 7.2 recorded at **a** Naf–TMS (1×10^{-6}–2×10^{-5} M [DA]), **b** Naf–TMS/$[Ru(phen)_3]^{2+}$ (7×10^{-8}–3×10^{-6} M [DA]) and **c** Naf–TMS/$[Ru(CN)_6]^{4-}$ (6×10^{-8}–3×10^{-6} M [DA])-modified glassy carbon electrodes. Scan rate, 20 mV s^{-1}; pulse amplitude, 50 mV; pulse duration, 200 ms. *Insets*, linear dependence of peak current on DA concentration

inset in Fig. 5a shows the linear response of the peak current with the concentration of DA. The sensitivity obtained from the slope was 0.1±0.01 μA/μM, and considering a (3×noise/sensitivity) ratio, the limit of detection was 0.1±0.01 μM, which is similar to that of Nafion®-modified electrodes after preconcentration [37] and that reported by Chen et al. [38] for mercaptopropylphosphonic acid-modified gold electrodes.

We are not sure about the mechanism according to which DA is easily oxidized on the Naf–TMS electrode. Since Naf–TMS is not a cation exchange polymer, we would expect that ionic exchange cannot be the reason to readily oxidize DA; instead we consider that the increase in sensitivity could be due mainly to hydrophobic interactions. It has been demonstrated that hydrophobic interactions are sufficiently strong even to compensate electrostatic repulsions of cationic DA with positively charged polymers (polydimethylaniline) as was reported before by Roy et al. [39]. Also, Vasantha and Chen [40] have observed the same phenomenon between a polymer film (poly(3,4-ethylendioxy)thiophene) and DA. Hydrophobic interactions have also been documented by Kumar and coworkers [41]. Through voltammetric studies, they found that DA adsorption is favoured in hydrophobic regions of polymers, increasing the DA oxidation current. The importance of hydrophobic interactions associated with the binding of cationic species to micellar media has also been apparent in systems where no electrostatic forces are present. Moreover, if we take into account the fact that the introduction of a trimethylsilyl group increases the hydrophobicity of the film, we expect that a hydrophobic environment facilitates the oxidation of DA by means of hydrophobic interactions. Nevertheless, we do not discard the possibility of electrostatic interactions since the very acidic SO_3 group of Naf–TMS could lodge part of the cationic DA^+ at this pH. In the next section, we present a study at different pH values to explore this assumption.

Loading Ru complexes into the Naf–TMS polymer further enhances the sensitivity and improves the detection limit to detect DA. This improvement can be attributed to an enhancement of the efficiency in charge hopping due to Ru redox centres within the film [36, 42, 43] or to additional negatively charged ion exchange sites in the film provided by the $[Ru(CN)]^{4-}$ sites. Differential pulse voltammograms obtained at neutral pH, with GC/Naf–TMS/$[Ru(phen)_3]^{2+}$ and GC/Naf–TMS/$[Ru(CN)_6]^{4-}$ electrodes, are shown in Fig. 5b, c, respectively, with the calibration plots presented as inset. Both modified surfaces exhibited a highly linear response (r=0.999±0.002) along two orders of magnitude of DA concentrations. The analytical and electrochemical parameters obtained are reported in Table 2.

From Fig. 5b, c, it can be clearly seen that both Ru complex-modified electrodes are rather sensitive to detect low concentrations of DA. At pH 7.2, they showed relatively identical characteristics and we did not observe any effect of the ligand attached to the metal ion (Ru) for the electrooxidation reaction. For both electrodes, the current detected was about eight times higher than that obtained with GC/Naf–TMS. A plot of the DA concentration versus the measured current is shown as inset in Fig. 5b, c for GC/Naf–TMS/$[Ru(phen)_3]^{2+}$ and GC/Naf–TMS/$[Ru(CN)_6]^{4-}$ electrodes, respectively. The slope of this plot is 0.83±0.02 μA/μM for the inset in Fig. 5b and 1.04±0.02 μA/μM for the inset in Fig. 5c. The corresponding detection limits obtained were 13±2 and 6±1 nM. These values were similar to those reported for other modified electrodes [44]. As can be seen, the detection limit of electrodes modified with $[Ru(CN)_6]^{4-}$ was slightly improved, which can be due to an electrostatic interaction between cationic DA^+ [45] and $[Ru(CN)_6]^{4-}$.

In an attempt to elucidate the role of ruthenium on the oxidation mechanism of the redox probe, we carried out experiments in the presence of low concentrations of dopamine and performed a study based on semiintegration analysis [46, 47]. Figure 6 (solid line) shows the cyclic voltammogram for the oxidation of 1 μM DA in phosphate buffer solution after baseline correction. The redox pair associated with the DA oxidation and reduction appeared at −0.213 V (±0.005) and −0.238 (±0.005) V, respectively. The high sensitivity of the electrode at low concentrations of analyte can be clearly observed. The voltammetric response obtained with the GC/Naf–TMS/$[Ru(phen)_3]^{2+}$ electrode indicates fast electron transfer kinetics for DA and a Nerstian behaviour since the

Table 2 Analytical parameters obtained from differential pulse and cyclic voltammetry using Naf–TMS and Naf–TMS/Ru complex-modified glassy carbon electrodes in the presence of several concentrations of dopamine (supporting electrolyte: phosphate buffer solution, pH 7.2)

Electrode modifier	[DA] 10^{-6} M	Sensitivity (μA/μM)	Detection limit (M)	ΔE^a (mV)	D (cm^2/s)
Naf–TMS	1.0–20.0	0.1±0.01	$1.0\pm0.01\times10^{-7}$	160±5	[b]
Naf–TMS/$[Ru(phen)_3]^{2+}$	0.08–3.0	0.83±0.02	$13.0\pm2\times10^{-9}$	77±2	$(2.8\pm0.4)\times10^{-7}$
Naf–TMS/$[Ru(CN)_6]^{4-}$	0.07–2.7	1.0±0.02	$6.0\pm1\times10^{-9}$	60±2	$(4.7\pm0.5)\times10^{-7}$

[a] Determined at 1.2×10^{-4} M DA by CV; scan rate, 100 mV s^{-1}

[b] Non-linear dependence of current vs square root of scan rate

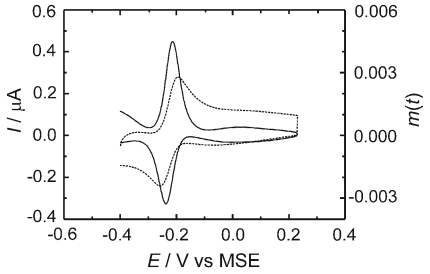

Fig. 6 Cyclic voltammogram for 1 μM DA in PBS pH 7.2 at Naf–TMS/Ru[(phen)$_3$]$^{2+}$-modified glassy carbon electrode. Scan rate, 100 mV s^{-1} (*black solid line*). The *dashed line* corresponds to the semiintegral analysis [46, 47] of the corresponding voltammogram

separation of peak potentials, ΔE, was only 0.025 V (it would be 0.030 V for a redox reaction involving two electrons [48]). With continuous scanning, ΔE remained constant. The results thus far indicate that electron transfer can occur rapidly on the GC/Naf–TMS/[Ru(phen)$_3$]$^{2+}$ electrode, even though DA is positively charged under these conditions. This result is supported by the observation that the electrostatic repulsion in the presence of cationic redox couples might be compensated by hydrophobic interactions between DA and the polymer films [39, 40]. The catalytic activity is attributed to a combination of chemical catalysis with redox mediation dictated by adsorption. Semiintegration of the DA voltammogram deviates from the ideal sigmoidal shape (Fig. 6, dashed line), where the current is diffusion-limited and exhibits a peak above the diffusion plateau. This points towards a process not entirely controlled by the diffusion of a charge transfer active species. Contribution due to the oxidation of adsorbed species, similar to that reported by Baur et al. [47] for DA in PBS pH 7.4, cannot be excluded.

Cyclic voltammograms in the presence of 118 μM DA in PBS pH 7.2 are shown in Fig. 7a–c for GC/Naf–TMS, GC/Naf–TMS/Ru[(phen)$_3$]$^{2+}$ and GC/Naf–TMS/Ru[(CN)$_6$]$^{4-}$ electrodes. For the GC/Naf–TMS surface, the redox pair associated to DA oxidation/reduction appears at −0.142 V (P1) and −0.302 V (P1′), respectively, leading to an ΔE value of 0.16±0.007 V. In contrast, for the GC/Naf–TMS/Ru[(phen)$_3$]$^{2+}$ electrode, the ΔE value decreased considerably (0.077±0.005 V, P2 and P2′). This clearly reflects the ruthenium effect to overcome the energy barrier to oxidize DA. Based on the results obtained by DPV, we expected a similar behaviour of the GC/Naf–TMS/[Ru(CN)$_6$]$^{4-}$ electrode to oxidize DA. As can be seen in Fig. 7c, DA oxidation and reduction occur at similar potentials compared to the GC/Naf–TMS/Ru[(phen)$_3$]$^{2+}$ electrode; we observed only a slight improvement in ΔE value (0.060± 0.003 V, P3 and P3′).

As is well known, DA at pH between 1 and 7 is found in the cationic form [45]. Since Ru[(phen)$_3$]$^{2+}$ and DA$^+$ are both positively charged, the electrostatic interaction cannot explain the improvement observed in the voltammetric

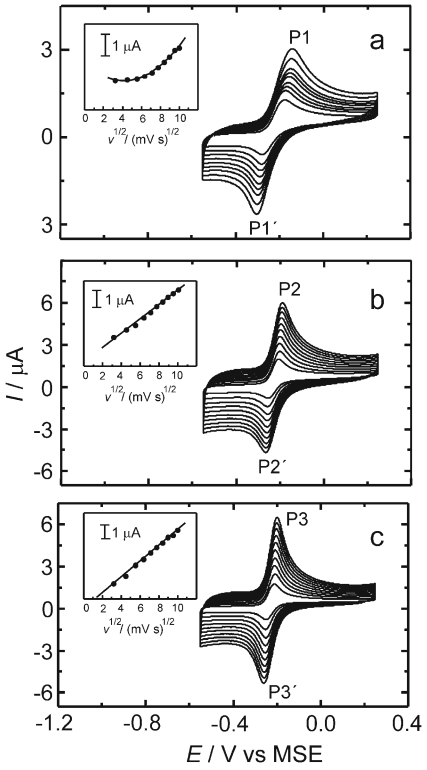

Fig. 7 Cyclic voltammograms recorded at different scan rates in the presence of 1.2×10^{-4} M DA in phosphate buffer solution at **a** Naf–TMS, **b** Naf–TMS/[Ru(phen)$_3$]$^{2+}$ and **c** Naf–TMS/[Ru(CN)$_6$]$^{4-}$-modified glassy carbon electrodes. *Insets*, dependence of anodic current peak on the square rate of the scan rate. Scan rates from 10 to 100 mV s^{-1}

response. Instead we consider that hydrophobic interactions are the reason. In Ru[(phen)$_3$]$^{2+}$, the charge is localized on the central metal ion, and the ligation sphere, which interacts with the solvating water molecules, is hydrophobic, favouring this kind of interaction. As mentioned above, it has been demonstrated that hydrophobic forces are sufficiently strong to compensate electrostatic repulsions [39, 49]. In the case of GC/Naf–TMS/[Ru(CN)$_6$]$^{4-}$ electrode, we suppose an electrostatic

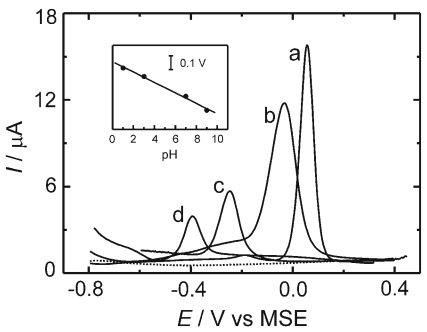

Fig. 8 Series of differential pulse voltammograms for a 20-μM DA recorded at several pH values: (*a*) 1, (*b*) 3, (*c*) 7, (*d*) 9 and 11 (*dashed line*) using a modified Naf–TMS glassy carbon electrode. Scan rate, 20 mV s^{-1}; pulse amplitude, 50 mV; pulse duration, 200 ms. *Inset*, dependence of anodic peak potential versus pH of the electrolyte

(and strong) interaction between cationic DA^+ and $[Ru(CN)_6]^{4-}$ anions, which can explain the further decrease in the ΔE values for the oxidation–reduction peaks.

Insets of Fig. 7 show the current response of the Naf–TMS and Naf–TMS/Ru complex electrodes in the presence of 118 μM DA at scan rates from 10 to 100 mV/s. Clearly, the GC/Naf–TMS surface does not follow a linear dependence of peak current to the square root of the scan rate. However, the response for Naf–TMS/Ru complex electrodes showed a good linear dependence as can be seen in insets of Fig. 7b, c. From the slope of these figures, the D of the reactant was calculated and the values were rather similar for both Ru-modified electrodes at $(2.8\pm0.4)\times10^{-7}$ and $(4.7\pm0.5)\times10^{-7}$ as observed in Table 2.

pH dependence on the analytical behaviour of Naf–TMS-modified glassy carbon electrode

As is well known, the electrochemical characteristics of catecholamine redox probes are pH dependent. This phenomenon arises from purely thermodynamic conditions but also would reflect the kind of interactions involved in the oxidation of dopamine. Figure 8 shows a series of differential pulse voltammograms recorded for 20 μM DA at various pH values using a GC/Naf–TMS electrode. As can be seen, the peak potential of the dopamine oxidation presents a pH dependence. A potential shift to more negative values occurs as the pH of the electrolyte increases, following a Nerstian behaviour expressed by the slope of the linear dependence of peak potential vs pH (shown as inset in Fig. 8). The slope of the line is −56 mV/pH unit, and from Nerst equation one would expect a slope of −59 mV/pH unit in a plot of E vs pH. This result gives us the idea that electrostatic interactions are also implicated in the oxidation of dopamine. At present, we are investigating the role of interfering substances and anions such as ascorbic acid and uric acid in the analytical response of dopamine. Afterwards, we will address the analytical capabilities of Naf–TMS and Naf–TMS/Ru complex-modified electrodes to other systems, for example, to detect heavy metal ions. This issue has been focused in a recent paper dealing with polyphenol-modified electrodes [50], which present excellent analytical properties.

Conclusions

We studied the nafion–trimethylsilyl resin and its modification with Ru complexes on glassy carbon electrodes and applied it for the study of DA oxidation in standard solutions. The results allow for some generalizations about the behaviour of Naf–TMS-modified glassy carbon electrodes. Naf–TMS membranes provide a short-time electrochemical response to detect cations. This response fluctuates depending on the intrinsic properties of the analytes. We found that differences in size, shape and hydrophobicity of the redox probes would lead to variations in the rate of diffusion trough the membrane. It was also found that the rate of the charge transfer process may involve hydrophobic and electrostatic interactions which would allow one to finely tune the properties of the membrane for possible analytical applications. The modification of Naf–TMS with Ru complexes further increased the rate of the charge transfer process and decreased the energy barrier for dopamine sensing. In-depth studies of the properties of Naf–TMS are underway to completely understand the charge transport mechanism in Naf–TMS and ruthenium-modified Naf–TMS membranes. These results will contribute to the wider use of nafion–TMS films as an electrode modifier in electrochemical applications and hopefully improve our understanding of non-covalent interactions of organic and hybrid species within membrane films.

Acknowledgements R.A.-S. and G. D.-M. greatly acknowledge support from PROMEP México (103.5/09/4194, 103.5/10/8442) and VIEP-BUAP 2010. Support from CONACyT-México under grants 90939 and 104361 is also acknowledged. R.A.-S. would like to thank Dr. M. Dávila for fruitful discussions.

References

1. Martin CR, Rubinstein I, Bard AJ (1982) J Am Chem Soc 104:4817–4824
2. Rubinstein I, Bard AJ (1980) J Am Chem Soc 102:6641–6642
3. Buttry DA, Anson FC (1982) J Am Chem Soc 104:4824–4829
4. Zheng L, Chi Y, Shu Q, Dong Y, Zhang L, Chen G (2009) J Phys Chem C 113:20316–20321
5. Tazi B, Savadogo O (2000) Electrochim Acta 45:4329–4339
6. Feng Z, Zhou J, Xi Y, Lan B, Guo H, Chen H, Zhang Q, Lin Z (2009) J Power Sources 194:1142–1149
7. White HS, Leddy J, Bard AJ (1982) J Am Chem Soc 104:4811–4817
8. Leddy J, Bard AJ (1985) J Electroanal Chem 189:203–219
9. Martin CR, Freiser H (1981) Anal Chem 53:902–904
10. George S, Lee HK (2009) J Phys Chem B 113:15445–15454
11. Kristensen EW, Kuhr WG, Wightman RM (1987) Anal Chem 59:1752–1757
12. Yeager HL, Steck A (1981) J Electrochem Soc 128:1880–1884
13. Zolfigol MA, Mohammadpoor-Baltork I, Habibi D, Mirjalili BF, Bamoniri A (2003) Tetrahedon Lett 44:8165–8167
14. Mauritz KA, Payne JT (2000) J Membr Sci 168:39–51
15. Murata S, Noyori R (1980) Tetrahedon Lett 21:767–768
16. Rubinstein I, Martin CR, Bard AJ (1983) Anal Chem 55:1580–1582
17. Wang S, Milam J, Ohlin AC, Rambaran VH, Clark E, Ward W, Seymour L, Casey WH, Holder AA, Miao W (2009) Anal Chem 81:4068–4075
18. Zen JM, Kumar AS, Chung CR (2003) Anal Chem 75:2703–2709
19. Yan X, Li H, Xu Z, Li W (2009) Bioelectrochemistry 74:310–314
20. Martin CR, Rhoades TA, Ferguson JA (1982) Anal Chem 54:1639–1641
21. Lowry SR, Mauritz KA (1980) J Am Chem Soc 102:4665–4667
22. Laporta M, Pegoraro M, Zanderighi L (1999) Phys Chem Chem Phys 1:4619–4628

23. Ostrowska J, Narebska A (1983) Colloid Polym Sci 261:93–98
24. Heitner-Wirguin C (1979) Polymer 20:371–374
25. Omberg KM, Schoonover JR, Bernhard S, Moss JA, Treadway JA, Kober EM, Dyer RB, Meyer TJ (1998) Inorg Chem 37:3505–3508
26. Diógenes ICN, Nart FC, Temperini MLA, Moreira IS (2001) Inorg Chem 40:4884–4889
27. Eller S, Schwarz P, Brimah AK, Fischer RD (1993) Organometallics 12:3232–3240
28. Hipps KW, Williams SD, Mazur U (1984) Inorg Chem 23:3500–3505
29. Assmann J, Narkhede V, Khodeir L, Löffler E, Hinrichsen O, Birkner A, Over H, Muhler M (2004) J Phys Chem B 108:14634–14642
30. Barton JK, Goldberg JM, Kumar CV, Turro NJ (1986) J Am Chem Soc 108:2081–2088
31. Yonemoto EH, Saupe GB, Schmeh RH, Hubig SM, Riley RL, Iverson BL, Mallouk TE (1994) J Am Chem Soc 116:4786–4795
32. Jenkins Y, Friedman AE, Turro NJ, Barton JK (1992) Biochemistry 31:10809–10816
33. Mandal K, Hauenstein BL Jr, Demas JN, DeGraff BA (1983) J Phys Chem 87:328–331
34. Bard AJ, Faulkner LR (1980) Electrochemical Methods. Wiley, New York, p 218
35. Yagi M, Kaneko M (2006) Adv Polym Sci 199:143–188
36. Kaneko M (2001) Prog Polym Sci 26:1101–1137
37. Nagy G, Oke GAG, Rice ME, Adams RN, Moore RB, Szentirmay MN, Martin CR (1985) J Electroanal Chem 188:85–94
38. Chen Y, Guo LR, Yang XJ, Jin B, Zheng LM, Xia XH (2009) Bioelectrochemistry 75:26–31
39. Roy PR, Okajima T, Ohsaka T (2003) Bioelectrochemistry 59:11–19
40. Vasantha VS, Chen SM (2006) J Electroanal Chem 592:77–87
41. Kumar SS, Mathiyarasu J, Phani KL (2005) J Electroanal Chem 578:95–103
42. Shiroishi H, Ishikawa K, Hirano K, Kaneko M (2001) Polym Adv Technol 12:237–243
43. Zhang J, Yagi M, Hou X, Kaneko M (1996) J Electroanal Chem 412:159–164
44. Hu G, Liu Y, Zhao J, Cui S, Yang Z, Zhang Y (2006) Bioelectrochemistry 69:254–257
45. Berfield JL, Wang LC, Reith MEA (1999) J Biol Chem 274:4876–4882
46. Bowling R, McCreery RL (1988) Anal Chem 60:605–608
47. Baur JE, Kristensen EW, May LJ, Wiedemann DJ, Wightman RM (1988) Anal Chem 60:1268–1272
48. Kissinger PT, Heineman WR (1983) J Chem Educ 60:702–706
49. Hackett JW, Turro C (1998) Inorg Chem 37:2039–2046
50. Oztekin Y, Yazicigil Z, Ramanaviciene A, Ramanavicius A (2011) Sensors and Actuators B Chem 152:37–48